

Permanent magnet synchronous motor control performed using PI-backstepping with a model of harmonics reduction

Ziani Said^{1,2}, Mohamed El Ghmary^{3,4}, Youssef Agrebi Zorgani^{5,6}

¹Laboratory of Networks, Computer Science, Telecommunication, Multimedia (RITM), Department of Electrical Engineering, High School of Technology ESTC, Hassan II University, Casablanca, Morocco

²Department of Health Technologies Engineering, Research Group in Biomedical Engineering and Pharmaceutical Sciences, ENSAM, Mohammed V University, Agdal, Morocco

³Department of computer science, Research Computer Sciences Laboratory (LRI), Intelligent Processing and Security of Systems (IPSS) Team, Faculty of Sciences, Mohammed V University, Rabat, Morocco

⁴Department of Computer Science, Faculty of Science, Dhar El Mahraz, Sidi Mohamed Ben Abdellah University, Fez, Morocco

⁵Laboratory of Sciences and Techniques of Automatic Control and Computer Engineering (Lab-STA),

National School of Engineering of Sfax, Sfax, Tunisia

⁶High Institute of Technological Studies of Sfax, Sfax, Tunisia

Article Info

Article history:

Received Dec 17, 2021

Revised Dec 4, 2022

Accepted Dec 17, 2022

Keywords:

Backstepping

Control

Disturbances

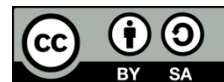
Lyapunov

Stability

ABSTRACT

This paper focuses on the control of permanent magnet synchronous motors (PMSMs) utilizing a non-linear adaptive PI-Backstepping design and a model of harmonics reduction approach that uses an active shunt filter followed by a cascade bandpass filter. While conventional backstepping may assure the system's stability, it is often imprecise. It creates a significant amount of static error, which has a detrimental effect on the system's behavior, such as disruptions and loads that might arise in industrial settings. We can assure minimum fixed errors and considerable interaction with uncertainty by integrating the PI controller with adaptive backstepping through robust Lyapunov functions. Numerical simulations are used to demonstrate the proposed controller's effectiveness.

This is an open access article under the [CC BY-SA](#) license.



Corresponding Author:

Ziani Said

Laboratory of Networks, Computer Science, Telecommunication, Multimedia (RITM)

Department of Electrical Engineering, High School of Technology ESTC, Hassan II University

Casablanca, Morocco

Email: ziani9@yahoo.fr

1. INTRODUCTION

The synchronous motor is generally used in three-phase power; it is reversible, that is, it can operate either as a generator or a motor. Most of the time, permanent magnet synchronous motors work the same way and perform the same way as regular synchronous motors. When a three-phase voltage source powers the stator, a rotating field is created in the air gap, rotating at a constant speed of $\omega = w/p$ revolutions per second, where w is the frequency of the stator power source and p is the number of pole pairs [1]. Due to their lack of rotor losses, resilience, and high specific power, synchronous machines with permanent magnets are increasingly used in speed variation. In contrast to the ease of connecting the thyristors in series, these machines may be provided with current inverters (based on thyristors) at extremely high power, and energy [2], [3]. In the literature, the permanent magnetic synchronous motor (PMSM) is controlled by a current switch (current control) and a voltage inverter, two different power supplies. Various control systems have different ways of changing the settings of the regulators in response to changes in the process being controlled. The methods that

came out of this are two simple adaptive techniques that have been widely used in practice. We were interested in building a modern control that utilized the backstepping idea in conjunction with integral proportional correction. The first section discusses the model of PMSM, specifically the mathematical model offered by a model of harmonics reduction strategy that employs an active shunt filter in conjunction with a cascade bandpass filter. Then, as a state representation, we determine the model of the PMSM and three-phase voltage inverter assembly [4]–[6]. The backstepping control of the PMSM [7]–[9] given by an inverter is determined. This section details the determination of current and speed regulators and examines the system's stability using Lyapunov's theory. The simulation results validate this sequence and demonstrate its performance and robustness to machine parameter fluctuations.

2. RESEARCH METHOD

The model of the synchronous motor PMSM and the research methodologies are discussed in this section. Simultaneously, the approximations for simplification are supplied [10].

2.1. Model

The PMSM model in the reference frame (d-q) is shown as follows:

$$\begin{cases} \frac{di_d}{dt} = -\frac{R_s}{L_d}i_d + p\frac{L_q}{L_d}\Omega i_q + \frac{v_d}{L_d} \\ \frac{di_q}{dt} = -\frac{R_s}{L_q}i_q - p\frac{L_d}{L_q}\Omega i_d - p\frac{\Omega\varphi_f}{L_q} + \frac{v_q}{L_q} \\ \frac{d\Omega}{dt} = \frac{p}{J}(L_d - L_q)i_d i_q - \frac{f}{J}\Omega + \frac{p}{J}\varphi_f i_q - \frac{C_r}{J} \end{cases} \quad (1)$$

where: R_s : Stator resistance (Ω), L_d, L_q : d,q axis self-inductance (H), φ_f : Mutual flux due to permanent magnetic (Wb), i_d, i_q : d,q axis currents (A), Ω Angle speed (rad/s), J : Moment of inertia (kg.m^2), f : damping constant (N/rad/s), p : Number of pole pairs, C_r : load torque (N.m).

As a result of the cross-coupling between the electrical current and speed state equations, the equations above indicate that PMSM is a highly nonlinear system. It should be noted that all characteristics fluctuate with operating circumstances, most notably the torque disturbance caused by the applied load, the temperature, and the saturation effects. Thus, if high-performance speed control of PMSM is required, the controller design must account for all nonlinearities, parameter uncertainties, and unknown external disturbances [11].

2.2. Backstepping control design

The primary control goal is to create an asymptotically stable speed tracking controller for PMSM that can accurately monitor the reference trajectory in the presence of all parameter uncertainties and perturbations and an unknown bounded load torque disturbance variation. This aim may be accomplished by designing the speed-tracking controller independent of all PMSM and load torque disturbance characteristics. So, it needs an adaptive online estimate of all parameters and disturbances from the outside. Adaptive backstepping tries to find a virtual control state and force it to act as a stabilizing function. This technique creates an error variable in the appropriate format [12]. Consequently, the error variable may be stabilized using the Lyapunov stability theory [13]–[16]. The overall control design can be made by following these three steps in order:

- Step 1: Define the reference speed as Ω^* and Ω^* as continuous second order derivatives. Moreover, the speed tracking error can be defined as:

$$z_\Omega = \Omega^* - \Omega + k_\Omega' \int_0^t (\Omega^* - \Omega) dt + \varepsilon \frac{\partial \Omega}{\partial t} \quad (2)$$

Where:

$$\varepsilon \xrightarrow[\varepsilon \in]{0} 0$$

So: $z_\Omega = e_\Omega + z_\Omega'$. Where: $e_\Omega = \Omega^* - \Omega$ and: $z_\Omega' = k_\Omega' \int_0^t (\Omega^* - \Omega) dt$ is the integral action added to the backstepping order to ensure convergence-tracking error towards zero despite uncertainties of type piecewise constant at each step of the algorithm. So, by using model (1), we find:

$$\dot{z}_\Omega = \dot{\Omega}^* - \dot{\Omega} + k_\Omega' (\Omega^* - \Omega) = \dot{\Omega}^* \left[\frac{p}{J}(L_d - L_q)i_d i_q - \frac{f}{J}\Omega + \frac{p}{J}\varphi_f i_q - \frac{C_r}{J} \right] + k_\Omega' (\Omega^* - \Omega) \quad (3)$$

Consider the first Lypanov function as:

$$V_{\Omega} = \frac{1}{2} z_{\Omega}^2$$

and the derivative of V_{Ω} is :

$$\dot{V}_{\Omega} = z_{\Omega} \dot{z}_{\Omega} = -K_{\Omega} z_{\Omega}^2$$

Then:

$$\dot{z}_{\Omega} = -K_{\Omega} z_{\Omega} = \dot{\Omega}^* - i_{q,ref} \left[(L_d - L_q) i_d + \varphi_f \right] \frac{p}{J} + \frac{f}{J} \Omega + \frac{c_r}{J} + k_{\Omega}' (\Omega^* - \Omega) \quad (4)$$

Finally, the virtual control $i_{q,ref}$ is given by the following equation:

$$i_{q,ref} = \frac{J}{p((L_d - L_q) + \varphi_f)} \left[\dot{\Omega}^* + \frac{c_r}{J} + \frac{f}{J} \Omega + K_{\Omega} z_{\Omega} + k_{\Omega}' (\Omega^* - \Omega) \right] \quad (5)$$

– Step 2: The i_q current tracking error can be defined to develop their dynamic:

$$z_q = i_{q,ref} - i_q + z_q'$$

So: $z_q = e_q + z_q'$. Where:

$$z_q' = k_q' \int_0^t (i_{q,ref} - i_q) dt + \varepsilon' \frac{\partial \Omega}{\partial t} \quad (6)$$

where:

$$\varepsilon' \xrightarrow[\varepsilon \in]{0,1[} 0 \text{ and: } e_q = i_{q,ref} - i_q$$

so:

$$\dot{z}_q = i_{q,ref} - i_q + k_q' (i_{q,ref} - i_q)$$

Define the second Lypanov function as:

$$V_q = V_{\Omega} + \frac{1}{2} z_q^2 + \frac{1}{2} z_q'^2$$

Then by using model (1), we find,

$$\dot{V}_q = -K_{\Omega} z_{\Omega}^2 + z_q [\dot{i}_{q,ref} - \dot{i}_q + k_q' (i_{q,ref} - i_q)] + z_q' \dot{z}_q'$$

Thus

$$V_q = -K_{\Omega} z_{\Omega}^2 + z_q [\dot{i}_{q,ref} - \dot{i}_q + k_q' (i_{q,ref} - i_q)] + z_q' k_q' (i_{q,ref} - i_q)$$

So, we get:

$$V_q = -K_{\Omega} z_{\Omega}^2 + z_q \left[\dot{i}_{q,ref} + \frac{R_s}{L_q} i_q + \frac{p\Omega}{L_q} \left(L_d i_d + \frac{\varphi_f}{L_q} \right) - \frac{v_{q,ref}}{L_q} + k_q' (i_{q,ref} - i_q) \right] + z_q' k_q' (i_{q,ref} - i_q)$$

We choose the control law to have:

$$\dot{V}_q = -K_{\Omega} z_{\Omega}^2 - k_q' z_q'^2 - (K_q - k_q') z_q^2 \leq 0 \quad (7)$$

Where: $(K_q - k_q') \geq 0$

Then:

$$\begin{aligned} \dot{V}_q = & -K_\Omega z_\Omega^2 + z_q \left[i_{q,ref} + \frac{R_s}{L_q} i_q + \frac{p\Omega}{L_q} \left(L_d i_d + \frac{\varphi_f}{L_q} \right) - \frac{v_{q,ref}}{L_q} + k_q' (i_{q,ref} - i_q) \right] + z_q (z_q - z_q') k_q' \\ & + z_q' k_q' (z_q - z_q') - K_q z_q = i_{q,ref} + \frac{R_s}{L_q} i_q + \frac{p\Omega}{L_q} \left(L_d i_d + \frac{\varphi_f}{L_q} \right) - \frac{v_{q,ref}}{L_q} \end{aligned}$$

Where:

$$v_{q,ref} = L_q \left[K_q z_q + i_{q,ref} + \frac{R_s}{L_q} i_q + \frac{p\Omega}{L_q} (L_d i_d + \varphi_f) \right] \quad (8)$$

– Step 3: The i_d current tracking error can be defined to develop their dynamic:

$$z_d = i_{d,ref} - i_d + k_d' \int_0^t (i_{d,ref} - i_d) dt \quad (9)$$

So:

$$z_d = e_d + z_d'$$

Where:

$$z_d' = k_d' \int_0^t (i_{d,ref} - i_d) dt$$

and

$$e_d = i_{d,ref} - i_d$$

Define the third Lyapunov function as:

$$V_d = \frac{1}{2} z_d^2 + \frac{1}{2} z_d'^2$$

Then:

$$\dot{V}_d = z_d \dot{z}_d + z_d' \dot{z}_d' = z_d [\dot{i}_d + k_d' (-i_d)] + z_d' (-k_d' i_d)$$

and by choosing:

$$i_{d,ref} = 0$$

We find:

$$z_d = -i_d + k_d' \int_0^t (-i_d) dt \Rightarrow z_d - z_d' = -i_d \Rightarrow i_d = z_d' - z_d$$

So, we get:

$$\dot{V}_d = -\dot{i}_d z_d - z_d k_d' i_d - k_d' z_d' i_d = -z_d \left(-\frac{R_s}{L_d} i_d + p \frac{L_q}{L_d} \Omega i_q + \frac{v_{d,ref}}{L_d} \right) + \alpha \quad (10)$$

where:

$$\alpha = -k_d' i_d (z_d + z_d') = k_d' (z_d + z_d') (z_d - z_d') = k_d' (z_d^2 - z_d'^2)$$

By using model (1) we find:

$$\dot{V}_d = -z_d \left(-\frac{R_s}{L_d} i_d + p \frac{L_q}{L_d} \Omega i_q + \frac{v_{d,ref}}{L_d} \right) + k_d' (z_d + z_d') (z_d - z_d')$$

So, by choosing:

$$\dot{V}_d = -(K_d - k_d') z_d^2 - k_d' z_d'^2$$

We get:

$$k_d' z_d^2 = z_d \left[-\frac{R_s}{L_d} i_d + p \frac{L_q}{L_d} \Omega i_q + \frac{v_{d,ref}}{L_d} \right] \quad (11)$$

and finally:

$$v_{d,ref} = L_d \left[K_d z_d + \frac{R_s}{L_d} i_d - p \frac{L_q}{L_d} \Omega i_q \right] \quad (12)$$

2.3. Model of harmonic reduction

Electrical machines can overheat when non-sinusoidal voltages are used. As long as the harmonic distortion doesn't go over the legal limit of 5%, motors run smoothly. They frequently encounter difficulties with overheating when they exceed this limit. Harmonic voltages or currents increase the stator and rotor winding losses. The losses caused by eddy currents and the skin effect are much less critical than those caused by the stator and rotor conductors [17]. For a machine driven by an inverter, the harmonic load losses were typically spread out as follows: 14.2% in the stator windings, 41.2% in the rotor bars, 18.8% in the end region, and 25.8% in the oblique flow. In practice, the harmonics to combat are those with odd ranks and low frequencies, particularly rows 3, 5, 7, 11, and 13. In the presence of harmonics, disruption of the speed or torque characteristics might result in machine malfunction. In Figure 1, we show how we want to connect cascading plug circuits to the PVM inverter in parallel with the network-tuning frequency needed for the motor to work.

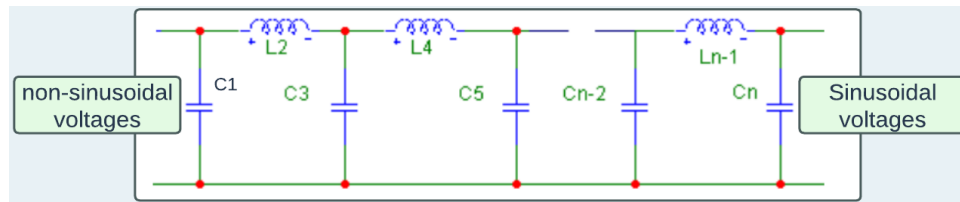


Figure 1. Harmonic filtering

3. RESULTS AND DISCUSSION

In this section, it is explained the results of the research and at the same time is given the comprehensive discussion.

3.1. Simulation of the control

The ratings and nominal parameters of the PMSM used in the simulations are given in Table 1. To validate the correctness and advantages of the proposed control strategies, and due to the lack of sufficient hardware in our laboratory to implement this complex control, the designed system is implemented using the MATLAB/Simulink package with SimPower Toolbox. In the simulation, the behavior of each method and its performances during the steady and transient states are analyzed to verify the effectiveness of the proposed backstepping control. Table 1 shows the gain values of the command used. The gains are adjusted according to the dynamics desired in a closed loop.

Table1. The nominal parameters and gain values

Parameter	Value	Parameter	Value
Kd	800	P	3
kq	800	R _s	0.2486 [Ω]
Kw	800	L _d	0.0023 [H]
Kdd	16	L _q	0.0028 [H]
Kqq	8	ϕ_f	0.19572 [Web]
Kww	10	J	0.005942 [N.mS ² /rad]
k_d'	Kdd	f	0.01124
k_q'	Kqq		
k_ω'	Kww		

3.1.1. Reference speed and load torque

The following figures illustrate the findings of the command by backstepping with integral action applied at the PMSM. The results are obtained with a perturbation due to the nominal load torque as shown in Figure 2(a) and amplitude of 5N.m. The objective is to control the closed-loop system's operation by first varying the rotational speed reference from 300 rad/s to 200 rad/s to 100 rad/s then to a final value equal to the rated speed: 50 rad/s as shown in Figure 2(b).

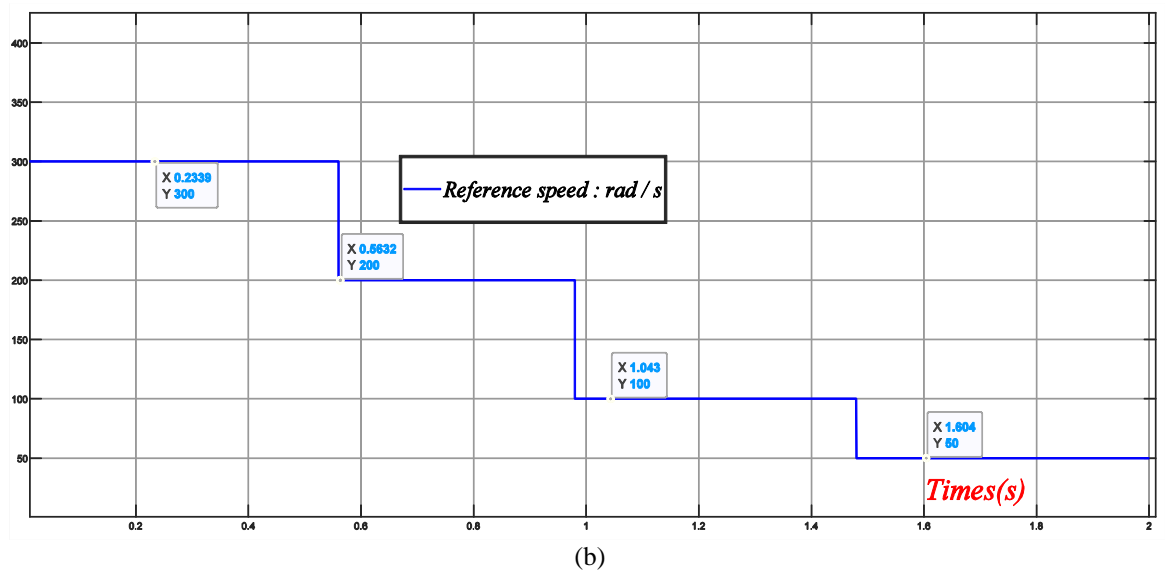
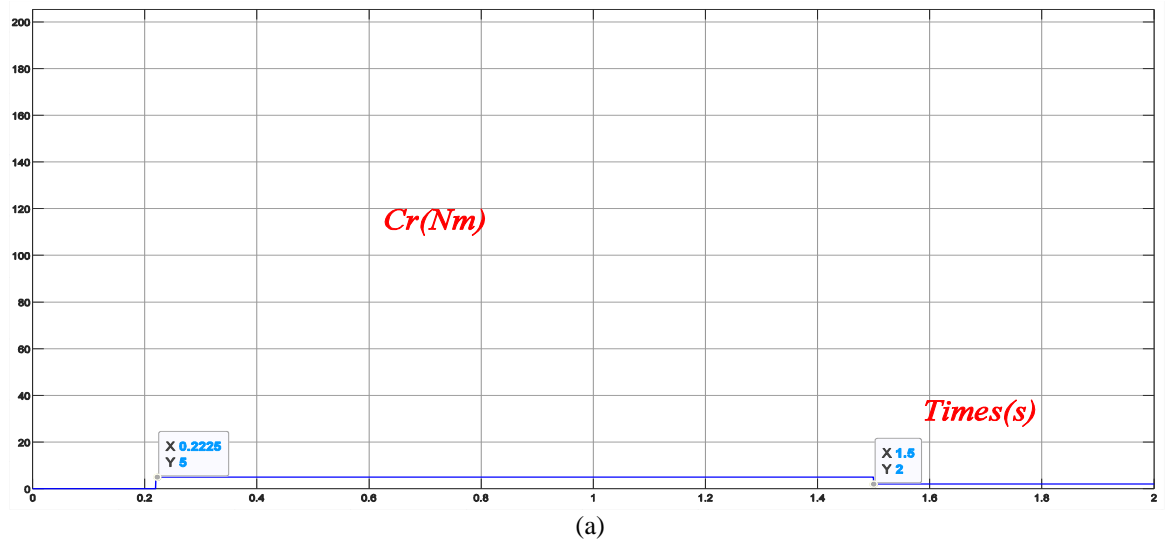


Figure 2. The command integral applied at the PMSM (a) load torque and (b) references speed

3.1.2. Simulation results

To demonstrate the command's efficiency and performance, we show simulation results in the following figures. The curves demonstrate the control's robustness in terms of load torque, resistance (100 per cent), and inductance (100 per cent) variation, as well as its efficiency when all parameters are varied. When all parameters are varied, the speed as shown in Figures 3(a) and 3(b) and Figures 4(a) and 4(b) converges towards its reference and the decoupling of the currents is maintained. The behaviour of electromagnetic torque is depicted as shown in Figures 5 (a) and (b).

3.2. Discussion of results

As noted in section 2.2, it is critical to ensure that the time derivative of the Lyapunov function candidate is negative semi-definite to maintain the asymptotic stability of the entire control system. The total

control system's asymptotic stability is then ensured. The simulation findings indicate that this essentiality is guaranteed in both circumstances. The proposed control's performance was evaluated using simulations for the classic adjustment of a PMSM supplied by a two-level voltage inverter, with a PI regulator facing a reference speed ranging from 100 to 300 (rad / s), followed by the application of a resistive torque of 5 (Nm) at a period of [1.27s], between $t = 0.22$ (s) and 1.449 (s). We denote a diligent pursuit of reference speed. The simulation results demonstrate that the decoupling is maintained regardless of the load variation. Since the inverter generates fluctuations that the cascaded bandpass filters reduce, they are not felt strongly at the torque level. After the transitory regime expires, the current Id value reverts to zero. The rate of change is rapid, with very little overshoot and no static inaccuracy. A 0.06-second optimal rising time also provides for speedy disturbance rejection (s). They also have a substantial impact on the estimate of several other factors. Parameter uncertainties/perturbations and load torque disturbance fluctuations are shown graphically in Figure 3.

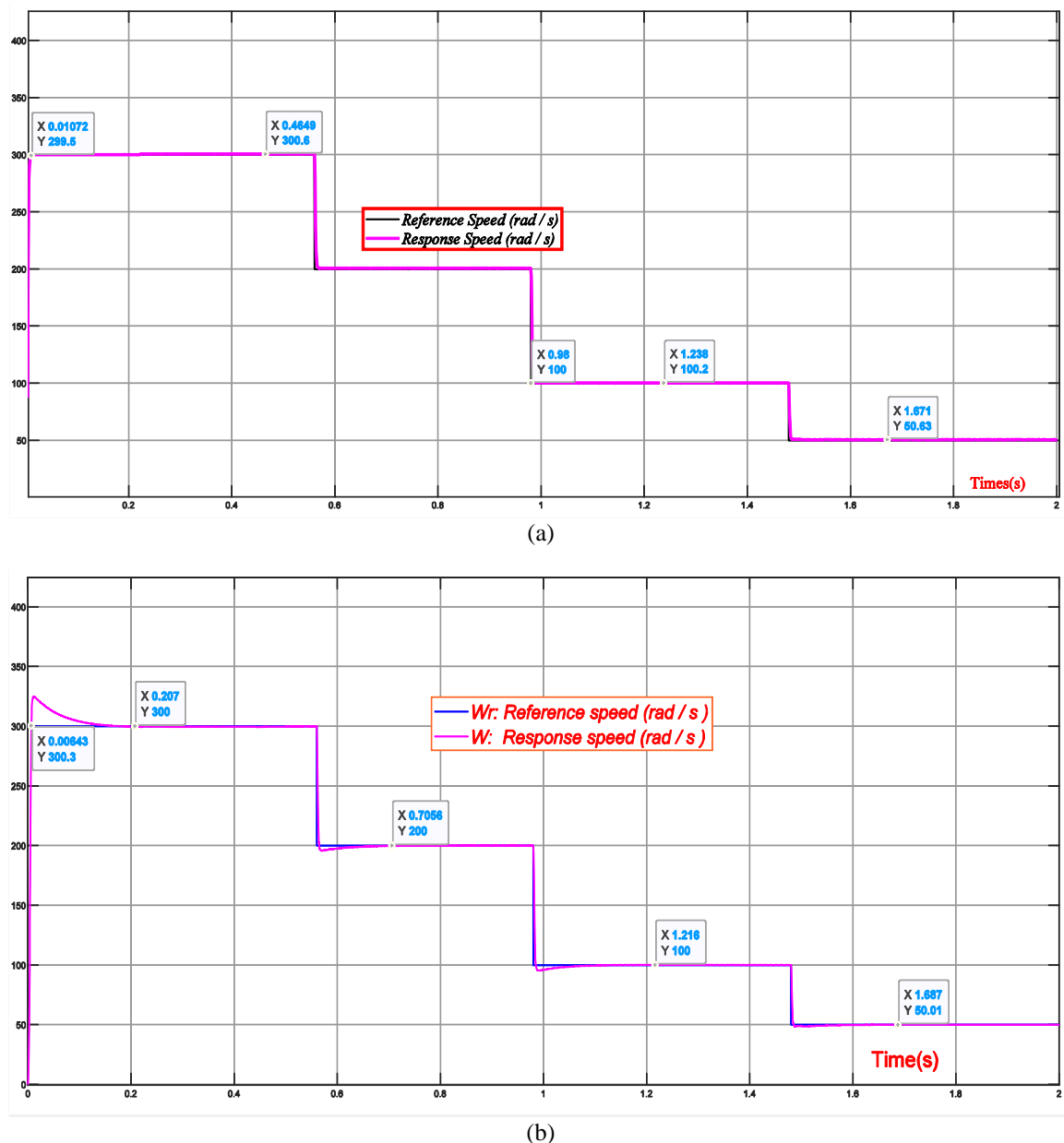


Figure 3. Response speed (a) for $K_{ww}=16$; $K_{qq}=8$; $K_{dd}=10$ and (b) for $K_{ww}=1.6$; $K_{qq}=0.8$; $K_{dd}=1$

Figures 4, and 5 demonstrate that the controller maintains a high level of robustness despite parameter uncertainties/apprehensions and load torque disturbance change. Compared with other recent works in the field [18]–[20], the presented approach is much more reliable and accurate. It is stated that the findings of this

study may be optimized utilizing a novel algorithm for mobile energy optimization by providing a heuristic solution based on the duties of the device [21]–[23]. The authors of [24] investigate the optimization of processing time and computing resources in a mobile edge computing node. Finally, this study's results highlight the integrated data analysis techniques often used in biomedical signal processing, such as ICA-NMF-SVD-PCA [25]–[28] with wavelets to further enhance the effectiveness of the methods as mentioned earlier.

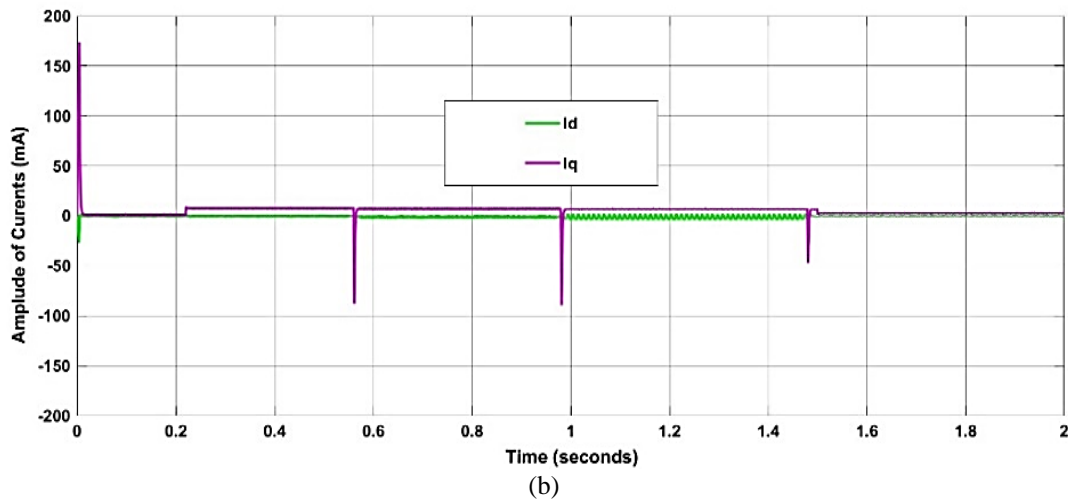
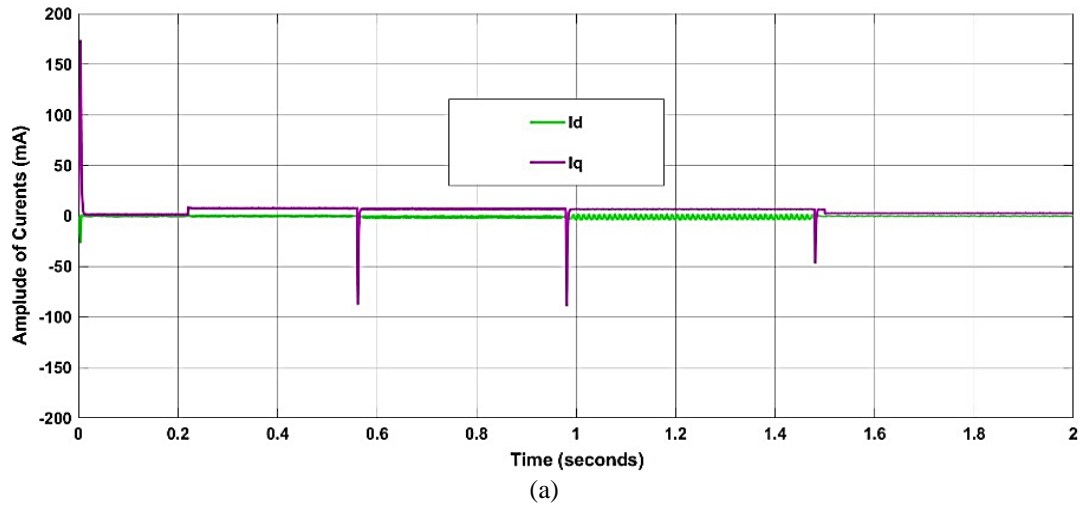


Figure 4. d_q axis Currents (a) for $K_{ww}=16$; $K_{qq}=8$; $K_{dd}=10$ and (b) for $K_{ww}=1.6$; $K_{qq}=0.8$; $K_{dd}=1$

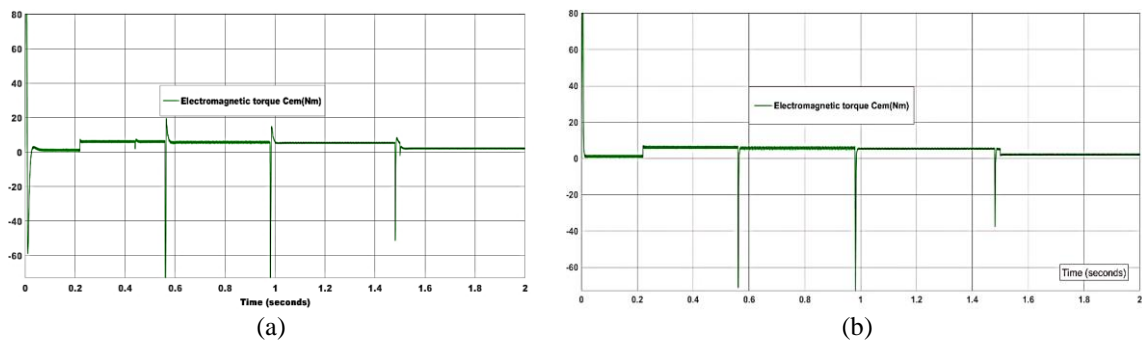


Figure 5. Electromagnetic torque (a) for $K_{ww}=16$; $K_{qq}=8$; $K_{dd}=10$ and (b) for $K_{ww}=1.6$; $K_{qq}=0.8$; $K_{dd}=1$

4. CONCLUSION

To improve the control's dynamic performance, we implemented an adaptive backstepping method. Each of the phases in the algorithm, as well as the stability analysis, have been discussed in detail. Proof of this method's worth lies in the fact that it permits adjustments to be made to the stator resistance, load torque, and inductors even when these parameters are not known. Results from the simulation agree with those predicted, proving the method to be successful. In conclusion, the findings of this study might be applied to prevent the failure of hybrid vehicles propelled by synchronous motors due to the excessively lengthy required ascent time.




REFERENCES

- [1] A. K. Shanshal, A. J. Ali, and A. H. Al-Rifaie, "Study the dynamic performance of PM machines for different rotor topologies," *International Journal of Power Electronics and Drive Systems*, vol. 13, no. 4, pp. 2062–2070, 2022, doi: 10.11591/ijpeds.v13.i4.pp2062-2070.
- [2] A. Boduroglu, Y. Demir, B. Cumhur, and M. Aydin, "A Novel Track Structure of Double-Sided Linear PM Synchronous Motor for Low Cost and High Force Density Applications," *IEEE Transactions on Magnetics*, vol. 57, no. 2, 2021, doi: 10.1109/TMAG.2020.3017448.
- [3] T. Li, X. Liu, and H. Yu, "Backstepping Nonsingular Terminal Sliding Mode Control for PMSM with Finite-Time Disturbance Observer," *IEEE Access*, vol. 9, pp. 135496–135507, 2021, doi: 10.1109/ACCESS.2021.3117363.
- [4] B. Liang, S. Zheng, C. K. Ahn, and F. Liu, "Adaptive Fuzzy Control for Fractional-Order Interconnected Systems with Unknown Control Directions," *IEEE Transactions on Fuzzy Systems*, vol. 30, no. 1, pp. 75–87, 2022, doi: 10.1109/TFUZZ.2020.3031694.
- [5] S. Rebouhl, A. Kaddouri, R. Abdessemed, and A. Haddoun, "Nonlinear control by input-output linearization scheme for EV permanent magnet synchronous motor," *VPPC 2007 - Proceedings of the 2007 IEEE Vehicle Power and Propulsion Conference*, pp. 185–190, 2007, doi: 10.1109/VPPC.2007.4544122.
- [6] M. A. Hamida, A. Glumineau, J. De Leon, and L. Loron, "Robust adaptive high order sliding-mode optimum controller for sensorless interior permanent magnet synchronous motors," *Mathematics and Computers in Simulation*, vol. 105, pp. 79–104, 2014, doi: 10.1016/j.matcom.2014.05.006.
- [7] J. Zhoua and Y. Wang, "Real-time nonlinear adaptive backstepping speed control for a PM synchronous motor," *Control Engineering Practice*, vol. 13, no. 10, pp. 1259–1269, 2005.
- [10] Y. Weng, D. Nan, and F. Wang, "Data-Driven Backstepping Sliding-Mode Control of Disturbed UAVs," *IEEE Access*, vol. 10, pp. 81713–81721, 2022, doi: 10.1109/ACCESS.2022.3196120.
- [11] M. Onsal, Y. Demir, and M. Aydin, "Impact of Asymmetric and Symmetric Overhangs on Torque Quality and Axial Magnetic Force Computations in Surface Mounted PM Synchronous Motors," *IEEE Transactions on Magnetics*, vol. 58, no. 2, 2022, doi: 10.1109/TMAG.2021.3090459.
- [12] S. Huang et al., "Fixed-Time Backstepping Fractional-Order Sliding Mode Excitation Control for Performance Improvement of Power System," *IEEE Transactions on Circuits and Systems I: Regular Papers*, vol. 69, no. 2, pp. 956–969, 2022, doi: 10.1109/TCSI.2021.3117072.
- [13] H. Gao, J. Zhu, X. Li, Y. Kang, J. Li, and H. Su, "Automatic Parking Control of Unmanned Vehicle Based on Switching Control Algorithm and Backstepping," *IEEE/ASME Transactions on Mechatronics*, vol. 27, no. 3, pp. 1233–1243, 2022, doi: 10.1109/TMECH.2020.3037215.
- [14] T. N. Truong, A. T. Vo, and H. J. Kang, "A backstepping global fast terminal sliding mode control for trajectory tracking control of industrial robotic manipulators," *IEEE Access*, vol. 9, pp. 31921–31931, 2021, doi: 10.1109/ACCESS.2021.3060115.
- [15] M. Wang, Z. Wang, H. Dong, and Q. L. Han, "A Novel Framework for Backstepping-Based Control of Discrete-Time Strict-Feedback Nonlinear Systems with Multiplicative Noises," *IEEE Transactions on Automatic Control*, vol. 66, no. 4, pp. 1484–1496, 2021, doi: 10.1109/TAC.2020.2995576.
- [16] F. Mazenc and P.-A. Bliman, "Backstepping Design for Time-Delay Nonlinear Systems," *IEEE Transactions on Automatic Control*, vol. 51, no. 1, pp. 149–154, Jan. 2006, doi: 10.1109/TAC.2005.861701.
- [17] Q. Du, L. Gao, Q. Li, T. Li, and F. Meng, "Harmonic Reduction Methods at DC Side of Parallel-Connected Multipulse Rectifiers: A Review," *IEEE Transactions on Power Electronics*, vol. 36, no. 3, pp. 2768–2782, 2021, doi: 10.1109/TPEL.2020.3013407.
- [18] D. Chen, K. Lu, D. Wang, and M. Hinkkanen, "A Small-signal Stability Study for Open-loop I-f Control of Permanent Magnet Synchronous Machine Drives," *2021 4th International Conference on Energy, Electrical and Power Engineering, CEEPE 2021*, pp. 405–409, 2021, doi: 10.1109/CEEPE51765.2021.9475661.
- [19] R. Zhang, Z. Yin, N. Du, J. Liu, and X. Tong, "Robust Adaptive Current Control of a 1.2-MW Direct-Drive PMSM for Traction Drives Based on Internal Model Control with Disturbance Observer," *IEEE Transactions on Transportation Electrification*, vol. 7, no. 3, pp. 1466–1481, 2021, doi: 10.1109/TTE.2021.3058012.
- [20] P. Yi, X. Wang, D. Chen, and Z. Sun, "PMSM Current Harmonics Control Technique Based on Speed Adaptive Robust Control," *IEEE Transactions on Transportation Electrification*, vol. 8, no. 2, pp. 1794–1806, 2022, doi: 10.1109/TTE.2021.3128535.
- [21] S. Manglik, A. Sen, B. Singh, and B. K. Panigrahi, "Low Power Sensorless PMBLDC Motor Drive with PFC for Domestic Flour Mill," *3rd International Conference on Energy, Power and Environment: Towards Clean Energy Technologies, ICEPE 2020*, 2021, doi: 10.1109/ICEPE50861.2021.9404433.
- [22] M. El Ghmary, M. O. C. Malki, Y. Hmimz, and T. Chanyour, "Energy and Computational Resources Optimization in a Mobile Edge Computing Node," *9th International Symposium on Signal, Image, Video and Communications, ISIVC 2018 - Proceedings*, pp. 323–328, 2019, doi: 10.1109/ISIVC.2018.8709200.
- [23] M. El Ghmary, T. Chanyour, Y. Hmimz, and M. O. C. Malki, "Efficient multi-task offloading with energy and computational resources optimization in a mobile edge computing node," *International Journal of Electrical and Computer Engineering*, vol. 9, no. 6, pp. 4908–4919, 2019, doi: 10.11591/ijece.v9i6.pp4908-4919.
- [24] P. Fajri, S. Heydari, and N. Lotfi, "Optimum low speed control of regenerative braking for electric vehicles," *2017 6th International Conference on Renewable Energy Research and Applications, ICRERA 2017*, vol. 2017-Janua, pp. 875–879, 2017, doi: 10.1109/ICRERA.2017.8191185.
- [25] S. Ziani and Y. El Hassouani, "Fetal-Maternal Electrocardiograms Mixtures Characterization Based on Time Analysis," *2019 International Conference on Optimization and Applications, ICOA 2019*, 2019, doi: 10.1109/ICOA.2019.8727619.




- [26] S. Ziani, A. Jbari, and L. Bellarbi, "QRS complex characterization based on non-negative matrix factorization NMF," *Proceedings of the 2018 International Conference on Optimization and Applications, ICOA 2018*, pp. 1–5, 2018, doi: 10.1109/ICOA.2018.8370548.
- [27] S. Ziani and Y. El Hassouani, "Fetal Electrocardiogram Analysis Based on LMS Adaptive Filtering and Complex Continuous Wavelet 1-D," *Lecture Notes in Networks and Systems*, vol. 81, pp. 360–366, 2020, doi: 10.1007/978-3-030-23672-4_26.
- [28] M. M. Akrofi and M. Okitasari, "Integrating solar energy considerations into urban planning for low carbon cities: A systematic review of the state-of-the-art," *Urban Governance*, 2022, doi: 10.1016/j.ugj.2022.04.002.

BIOGRAPHIES OF AUTHORS






Prof. Dr. Ziani Said    is a professor at the Department of Electrical Engineering at Hassan II University (ESTC) in Casablanca, Morocco. He is with also Health Technologies Engineering Department, Research Group in Biomedical Engineering and Pharmaceutical Sciences, ENSAM, Mohammed V University, Agdal, Morocco His research interests include digital design, industrial applications, industrial electronics, industrial informatics, power electronics, motor drives, renewable energy, FPGA and DSP applications, embedded systems, adaptive control, neural network control, automatic robot control, motion control, and artificial intelligence. He is a senior Member of IEEE with Member/Customer Number: 98711129. He can be contacted at email: said.ziani@univh2c.ma or ziani9@yahoo.fr.



Mohamed El Ghmary    is a Professor of Computer Science at the Faculty of Sciences Dhar El Mahraz (FSDM), Sidi Mohamed Ben Abdellah University, Fez, Morocco. He is an associate member of Research Computer Sciences Laboratory (LRI), Team Intelligent Processing and Security of Systems (IPSS)) of Computer Science Department at the Faculty of Sciences, Mohamed V University (UM5), Rabat Morocco. He is also an associate member of Research Laboratory in Computer Science and Telecommunications (LARIT), Team Networks and Telecommunications, Faculty of Sciences, Ibn Tofail University, Kenitra, Morocco. His research interests are in Mobile Edge Computing (MEC), Cloud Computing, Machine Learning, Deep Learning, Intelligent Systems and Optimization. He can be contacted at email: mohamed.elghmary@usmba.ac.ma.



Dr. Youssef Agrebi Zorgani    is a full-time Professor in the electronics and power drive at the Department of Mechanical Engineering and at the Higher Institute of Technological Studies of Sfax, Tunisia. Dr. Youssef Agrebi Zorgani received his Ph.D. degree in Electrical Engineering from the National School of Engineering of Sfax (ENIS)-Tunisia and Ph.D. degree in Automatic from the Faculty of Science, University of d'Aix-Marseille – France. Dr. Youssef AGREBI ZORGANI has published 30+ papers and 1 book in the field of power Electronics and Motor Drive. He is a Member of Laboratory of Sciences and Techniques of Automatic control and computer engineering Lab-STA (ENIS, Sfax, Tunisia). Dr. Youssef Agrebi Zorgani actively serves as a reviewer in several journals and conference publications, including IEEE conferences and journals. He is the ECONOV'2022 International Conference on Ecological Innovation Chairman for 2022. His research interests focus on Electrical Power Engineering, Electrical & Electronics Engineering, Power Electronics, Renewable Energy, and Control systems. He can be contacted at email: agrebi69@yahoo.fr.